International Journal of Biological Macromolecules 318 (2025) 144889

Contents lists available at ScienceDirect

International Journal of Biological Macromolecules

journal homepage: www.elsevier.com/locate/ijbiomac

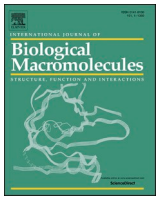

Seeking standardized *in vitro* models of AGE-RAGE signaling in the physiological perspective of glycated dietary proteins

Fleur A.C. Jansen [a,*], Josep Rubert [a,b], Klaske van Norren [b], Vincenzo Fogliano [a], Tamara Hoppenbrouwers [a,c]

[a] Department of Food Quality and Design, Wageningen University and Research, Bornse Weilanden 9, 6708 WG Wageningen, the Netherlands
[b] Department of Nutritional Biology, Division of Human Nutrition, Wageningen University and Research, Stippeneng 4, 6708 WE Wageningen, the Netherlands
[c] Food and Biobased Research, Wageningen University and Research, Bornse Weilanden 9, 6708 WG Wageningen, the Netherlands

ARTICLE INFO

Keywords:
Cell culture
Receptor for advanced glycation end products (RAGE)
Diet
Glycation
Inflammation
Endotoxin

ABSTRACT

Introduction: Advanced Glycation End products (AGEs) are covalent protein adducts formed through the Maillard reaction. High dietary intake might harm human health, however studies on their impact remain inconclusive. A proposed mechanism is that dietary AGEs trigger inflammation by interacting with the AGEs receptor (RAGE). However, *in vitro* studies on dietary AGE-RAGE signaling have reported inconsistent results, probably due to methodological issues. This study aimed to seek a standardized model of dietary AGE-RAGE signaling.
Methods: In vitro models were characterized for surface and total RAGE expression using flow cytometry. Both commercially available and in-house prepared dietary AGE preparations were analyzed for AGE levels, aggregation, and LPS content, then tested in the model with the highest surface RAGE expression.
Results: All immortalized cell lines expressed intracellular RAGE, while its surface expression was marginal or even absent. Only M-CSF-differentiated M0 macrophages showed significant surface RAGE expression. Some glycated dietary proteins induced inflammation in this model, but not all. While these proteins showed RAGE affinity in a chemical assay, the inflammatory response could not be reduced by the RAGE antagonist FPS-ZM1. Interestingly, co-incubation with the LPS scavenger PMB reduced inflammation despite negligible LPS levels in the sample.
Conclusion: These results challenge the hypothesis that dietary AGEs cause inflammation *via* RAGE activation, as glycated dietary proteins alone do not seem to induce acute inflammation. To better understand the biological activity of dietary AGEs, future studies should confirm surface RAGE expression, detail glycation methods and glycated protein characteristics, and account for LPS interference.

1. Introduction

Advanced Glycation End products (AGEs) are a heterogeneous group of covalent adducts and cross-linking structures in proteins formed by the Maillard Reaction. This reaction, also known as protein glycation, is a non-enzymatic process in which carbonyl groups of reducing sugars react with free amino groups of proteins, namely the side chain of lysine or arginine residues [1]. Since the Maillard Reaction happens non-enzymatically, it is driven by moderately high temperature, but the formation of AGEs also happens continuously on body proteins, although at low velocity. The concentration of AGEs in tissues such as articular collagen and the lens increases with age and was shown to be higher in diabetics [2–4]. This accumulation has been linked to many age-related non-communicable diseases, like cataract and cardiovascular diseases, and diabetes-related complications [1–3].

Multiple mechanisms have been described through which glycation contributes to such disease states. These mechanisms include for example the formation of protein crosslinks, inducing structural changes and possibly affecting protein functionality [1]. In addition, the interaction between AGEs and the AGEs receptor (RAGE) is often mentioned [5–7]. This receptor was first described three decades ago when researchers were searching for recognition sites for AGEs on the cell surface [8,9]. RAGE is a member of the immunoglobulin superfamily of cell surface molecules with a multiligand character [10]. This implies that not only AGEs but also other ligands, mainly damage-associated molecular patterns, can bind to the extracellular region of this

* Corresponding author at: Bornse Weilanden 9, 6708 WG Wageningen, the Netherlands.
E-mail address: fleur.jansen@wur.nl (F.A.C. Jansen).

https://doi.org/10.1016/j.ijbiomac.2025.144889
Received 8 January 2025; Received in revised form 22 April 2025; Accepted 2 June 2025
Available online 2 June 2025

transmembrane receptor. Especially the V-domain of the extracellular part of RAGE is involved in the recognition of these ligands. When the receptor gets activated by the binding of a ligand, its cytoplasmic tail initiates an intracellular signaling cascade leading to the production of pro-inflammatory cytokines. Multiple pathways are involved in this signaling cascade, with the NFκB pathway playing a pivotal role [7]. These series of events starting with AGEs binding to RAGE and ending with the production of pro-inflammatory cytokines is often referred to as AGE-RAGE signaling [11–13].

According to some scholars, dietary AGEs can also trigger AGE-RAGE signaling and high intake of food rich in dietary AGEs would be harmful for human health. Human observational and intervention studies are however inconclusive and the most recent intervention trial failed to find any correlation between the intake of dietary AGEs and several health outcomes [14,15]. When comparing dietary AGEs to endogenous AGEs, a few structural differences can be stated [16], however the main point is the bioactivity of glycated dietary proteins being affected by their digestion, absorption, distribution, metabolism and excretion. The majority of the dietary AGEs will be absorbed as single amino acids, di- or tripeptides, while a relatively large peptide backbone is required for AGEs to bind to RAGE [17,18]. Therefore, dietary AGE-RAGE interaction could only occur at the intestinal level, or with cells of the intestinal immune system if part of the undigested protein fraction is able to pass the epithelial layer through paracellular transport and/or transcytosis [19–21]. To explore the consequences of dietary AGE-RAGE interaction, *in vitro* models are a frequently used tool. Currently, mixed results have been reported in this regard. Some studies indeed attribute pro-inflammatory properties to dietary AGEs [22–24], whereas other studies show no effect [25,26]. In general, these studies are hard to compare since they did not only investigate different proteins and use different glycation methods, but also tested these glycated proteins in different *in vitro* models. The objective of this study was to seek a standardized *in vitro* model of dietary AGE-RAGE signaling, to enhance our understanding of the biological activity of glycated dietary proteins. We hypothesized that differences in RAGE expression between models and in LPS content between samples are factors to consider.

In this study, different *in vitro* models were characterized using flow cytometry for their surface and total RAGE expression. Inflammatory properties of both commercially available and in-house dietary AGEs preparations (characterized for AGE levels, aggregation, and LPS content) were tested in the model showing highest surface RAGE expression. A RAGE antagonist and an LPS scavenger were included to check the actual involvement of AGE-RAGE signaling when a specific dietary AGEs preparation showed pro-inflammatory properties.

2. Results

2.1. Various immortalized cell lines primarily express RAGE intracellularly

To verify and validate the presence of RAGE at the cell surface, as depicted in the AGE-RAGE signaling hypothesis, its expression was measured using flow cytometry in six immortalized human cell lines (HMC3, THP-1, hCMEC/D3, HBVP, Raji, and Caco-2), that were previously described to express RAGE. An antibody specific for the V-domain of RAGE (epitope mapped by the manufacturer) was used on intact cells to identify RAGE when present as a cell surface receptor. The same protocol was used on fixated and permeabilized cells to also detect intracellular RAGE (total RAGE). Fig. 1A shows that, for all cell lines, only a small percentage of cells, ranging from 1.0 to 10.4 %, expressed RAGE on its surface. When considering total RAGE expression, this percentage clearly increased and varied from 71.1 to 99.3 %. When looking at the fluorescent intensity emitted, *i.e.* the relative expression level of RAGE per cell, expressed as the median fluorescent intensity (MFI), a similar trend between surface *vs.* total RAGE was observed: low relative expression level of surface RAGE (62 to 1362 RFU) compared to total RAGE (6356 to 180,000 RFU) (Fig. 1B). Therefore, these data show that RAGE was constitutively expressed intracellularly in immortalized cells while the surface expression only occurred marginally or was even absent.

2.2. Primary monocytes differentiated with M-CSF show increased surface RAGE expression

Next, RAGE levels were determined on primary monocytes, GM-CSF differentiated M0 macrophages, and M-CSF differentiated M0 macrophages. The results are shown in the different panels of Fig. 2. A substantial amount of primary monocytes was positive for total RAGE (79.3 ± 21.8 %), whereas monocytes expressing RAGE on their surface were more scarce (24.4 ± 29.4 %) (Fig. 2A). Differentiation to macrophages did subsequently not affect the percentage of cell positive for total RAGE ($P = 0.199$), while M-CSF differentiation significantly enhanced the percentage of cells expressing RAGE on its surface (24.4 ± 29.4 % *vs* 68.2 ± 16 %, $P = 0.027$). GM-CSF differentiation did not exert this effect (10.8 ± 6.5 % *vs* 24.4 ± 29.4 %, $P = 0.645$). In terms of relative expression levels (Fig. 2B), the enhancing effect of M-CSF differentiation was observed for both total (240 % increase, $P = 0.012$) and surface RAGE (1118 % increase, $P = 0.003$). With GM-CSF differentiation, no significant changes in the relative expression levels of total or surface

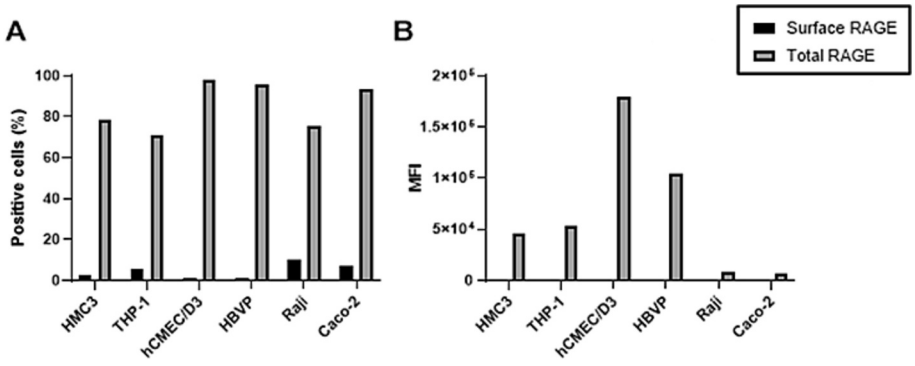

Fig. 1. *Percentage of positive cells (A) and median fluorescent intensity (MFI) (B) for RAGE measured on the cell surface (black bars) or in totality (grey bars) in different immortalized human cell lines: HMC3 (microglia), THP-1 (monocytes; differentiated to M0 macrophages), hCMEC/D3 (brain endothelial cells), HBVP (brain vascular pericytes), Raji (lymphoblasts) and Caco-2 (intestinal cells).* Flow cytometry analysis was performed on cells being fixed and permeabilized to assess total RAGE expression, whereas fixation and permeabilization steps were not applied when assessing surface RAGE expression. All values are relevant to (%) or corrected for (MFI) the unstained control, which implies no staining with the primary RAGE antibody.

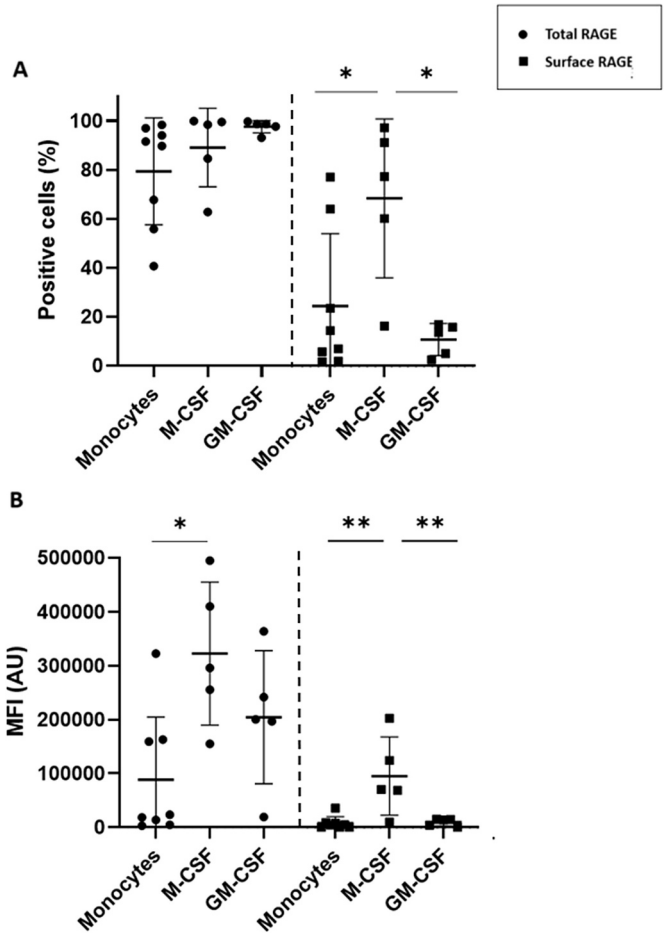

Fig. 2. *Percentage of positive cells (A) and median fluorescent intensity (MFI) (B) for RAGE in primary monocytes, M-CSF differentiated M0 macrophages, and GM-CSF differentiated M0 macrophages measured in totality (dots) and on the cell surface (squares).* Flow cytometry analysis was performed on cells being fixed and permeabilized to assess total RAGE expression, whereas fixation and permeabilization steps were not applied when assessing surface RAGE expression. All values are relevant to (%) or corrected for (MFI) the unstained control, which implies no staining with the primary RAGE antibody. Values are depicted as mean ± SD of biological replicates. *P*-values (* < 0.05, ** < 0.01) are obtained by a multiple comparisons test (Tukey) following ANOVA.

RAGE were observed (resp. $P = 0.254$ and $P = 0.996$). All in all, these data showed that primary monocytes express RAGE, but only sporadically on the cell's surface. With M-CSF differentiation, both the percentage of cells expressing surface RAGE as well as its relative expression level increased. This effect proved to be growth factor specific, since it was not observed for GM-CSF. Therefore, the M-CSF differentiated M0 macrophages can be considered a suitable *in vitro* model to study the function of RAGE as a multi-ligand cell surface receptor.

2.3. Prolonged heating of beta-lactoglobulin with glucose increases its glycation and aggregation levels

A common dietary protein, BLG, was heated with glucose for a prolonged time and characterized for glycation and aggregation levels before testing its inflammatory potential *in vitro*. This chemical characterization of the glycated BLG is reported in Fig. 3. These data indicate that the intact lysine content of BLG dropped upon glycation in a time-dependent manner, reaching a maximum of about 50 % after 12 h. As expected, with the decrease in intact lysine content, the levels of Amadori products (glucosyl-lysine detected as furosine) and AGEs (CEL and CML) increased, as they are formed on lysine residues. Glycation increased furosine and CEL levels over time up to respectively 33.1 μg/mg protein and 838.1 ng/mg protein, compared to resp. 1.8 μg/mg protein and 75.8 ng/mg protein under similar heating conditions. For CML, this difference between heating and glycating conditions was less pronounced, but its level still increased by 45 % upon glycation. This result indicates that a substantial amount of the available lysine in the glycated BLG used in the following biological experiments was modified due to the glycation. To quantify this level, based on the data of Fig. 3, the furosine-to-lysine ratio of the glycated samples was determined to be 20–26 %. This suggests an estimate average of approximately 3–4 sugar molecules attached per molecule of BLG. The SDS-PAGE gel pattern in Fig. 4 showing a slight increase in weight of the BLG monomer upon glycation also indicates the formation of AGEs. Furthermore, the number of high molecular weight structures increased over time, demonstrating the aggregation of BLG upon heating. In the presence of glucose, the formation of dimers and high molecular weight aggregates was more pronounced, indicating that glycation accelerates this aggregation process. This phenomenon was particularly evident after 24 h of heating with glucose. Combined with the furosine-to-lysine ratio of this sample, results indicate a high degree of glycation.

2.4. High levels of glycation and aggregation in beta-lactoglobulin correspond to an increased affinity to sRAGE

Next, a competitive sRAGE ELISA was performed with these BLG preparations to investigate their affinity to the receptor in the context of AGE-RAGE signaling. Aβ-42, a well-known RAGE ligand, was used as a positive control for sRAGE binding. Fig. 5 indicates that the native and all the heated BLG control samples had inhibition values below the detection limit (<25 %), whereas the glycated BLG samples dose-dependently inhibited the binding of sRAGE to the plate. As expected, inhibition values increased with prolonged heating time. In combination with the results discussed above regarding the glycation level and aggregation pattern of these preparations (Figs. 3 and 4), it can be argued that the higher the modification level of BLG, the higher its affinity to sRAGE. Accordingly, the BLG preparation that was glycated for 24 h was used in the *in vitro* experiments hereafter (Figs. 6, 7 and 8) as it most closely resembled the sRAGE binding capacity of Aβ-42.

2.5. Glycated BLG acts pro-inflammatory on surface RAGE-expressing M-CSF differentiated M0 macrophages

To investigate the activation of surface RAGE by dietary AGEs, M-CSF differentiated M0 macrophages were exposed for 24 h to our model sample, 24 h glycated BLG. Experimental data are reported in the different panels of Fig. 6. Cell viability was not affected (Fig. 6A, $P = 0.287$), while the excretion of several pro-inflammatory cytokines increased in a concentration-dependent manner ($P < 0.001$) (Fig. 6B, C and D). For IL-8, the concentrations dose-dependently increased up to 37.5 ± 13.0 ng/mL, when exposed to 1000 μg/mL glycated BLG ($P < 0.001$; compared to medium control). For IL-6 and TNFα, maximum concentrations of resp. 207.5 ± 86.0 pg/mL and 320.2 ± 38.6 pg/mL were detected (resp. $P < 0.001$ and $P < 0.01$; compared to medium control). Interestingly, although RAGE is not expressed on the surface of GM-CSF differentiated M0 macrophages, the glycated protein also induced a pro-inflammatory response in this *in vitro* model (data not

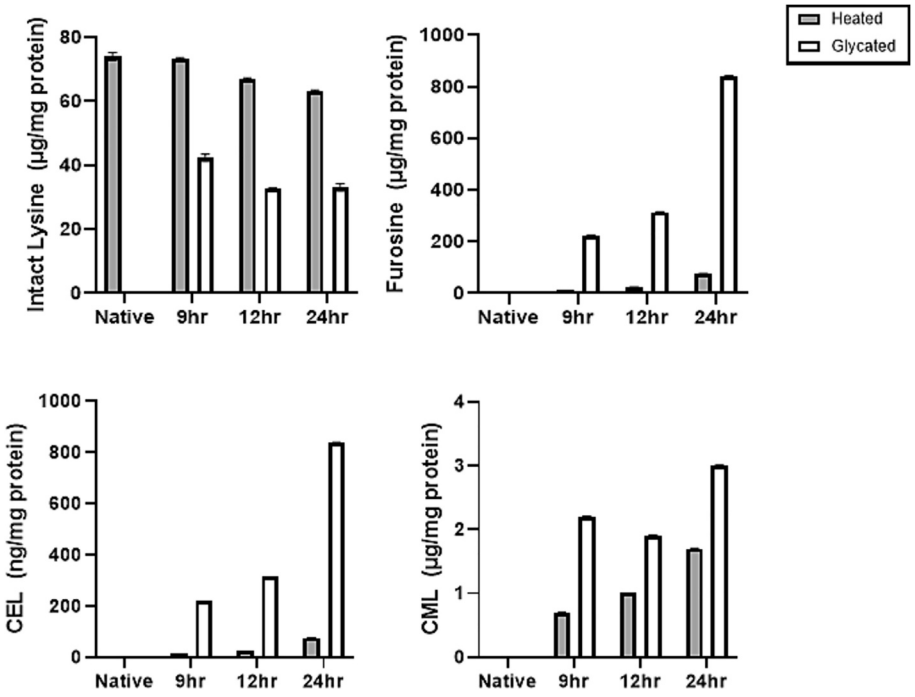

Fig. 3. *Levels of intact lysine, CEL, CML and furosine quantified by LC-MS/MS in beta-lactoglobulin (BLG).* BLG was dry heated with glucose for 9, 12 or 24 h at 60 °C and 40 % humidity (glycated) and compared to non-heated BLG (native) and BLG dry heated at similar conditions but without glucose (heated). Data is mean values±SD obtained from a technical duplicate.

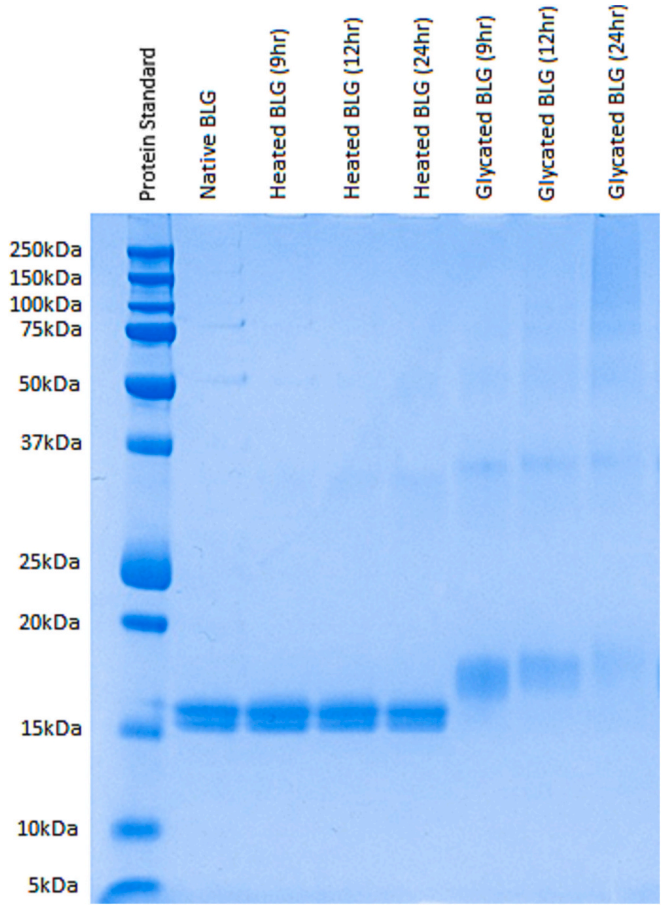

Fig. 4. *SDS-PAGE profile of Beta-Lactoglobulin (BLG).* BLG was dry heated with glucose for 9, 12 or 24 h at 60 °C and 40 % humidity (glycated) and compared to non-heated BLG (native) and BLG dry heated at similar conditions but without glucose (heated).

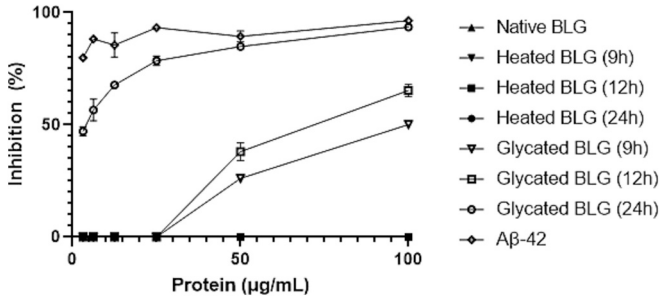

Fig. 5. *Inhibition ELISA for binding of Beta-Lactoglobulin (BLG) to sRAGE.* BLG was dry heated with glucose for 9, 12 or 24 h at 60 °C and 40 % humidity (glycated), and compared to non-heated BLG (native) and BLG dry heated at similar conditions but without glucose (heated). Aβ-42 was included as positive control. All compounds were tested in duplicate as a two-times dilution series from 100 µg/mL to 3.125 µg/mL. Data is mean values±SD obtained from a technical duplicate.

shown). This suggests mechanisms other than surface RAGE activation being involved.

2.6. The RAGE antagonist FPS-ZM1 does not inhibit the inflammatory effect of glycated BLG

Subsequently, M-CSF differentiated M0 macrophages were pre-incubated with a RAGE antagonist to confirm the involvement of RAGE in the observed pro-inflammatory response. The inhibitor FPS-ZM1 did not affect cell viability or act pro-inflammatory at the concentrations used (Supplementary Fig. 1). Data reported in Fig. 7 showed that FPS-ZM1 could not block the inflammatory effect. Neither IL-6, IL-8, nor TNFα secretion was lowered when the cells were pre-incubated for 1 h with this inhibitor (0-20 µM) prior to exposure to the glycated protein (200 µg/mL). Based on this data, surface RAGE does not seem to be involved in the observed pro-inflammatory response, despite the

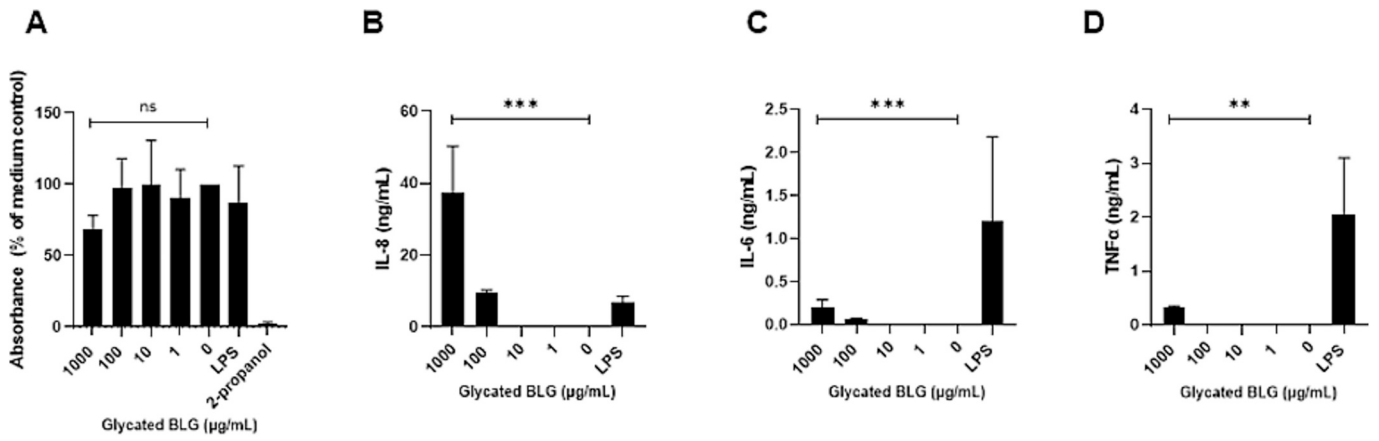

Fig. 6. *Cell viability of M-CSF differentiated M0 macrophages and their IL-8 (B), IL-6 (C) and TNFα (D) secretion upon exposure to glycated beta-lactoglobulin (BLG).* BLG was dry heated with glucose for 24 h at 60 °C and 40 % humidity. Subsequently, M-CSF differentiated monocytes were exposed to this glycated protein for 24 h at 37 °C (5 % CO_2, saturated humidity) at concentrations ranging from 1000 µg/mL to 1 µg/mL. LPS (100 ng/mL) was included as positive control. Data is mean values ± SD obtained from independent experiments performed with three different donors. P-values (** < 0.01, *** < 0.001) are obtained by a multiple comparisons test (Tukey) following ANOVA.

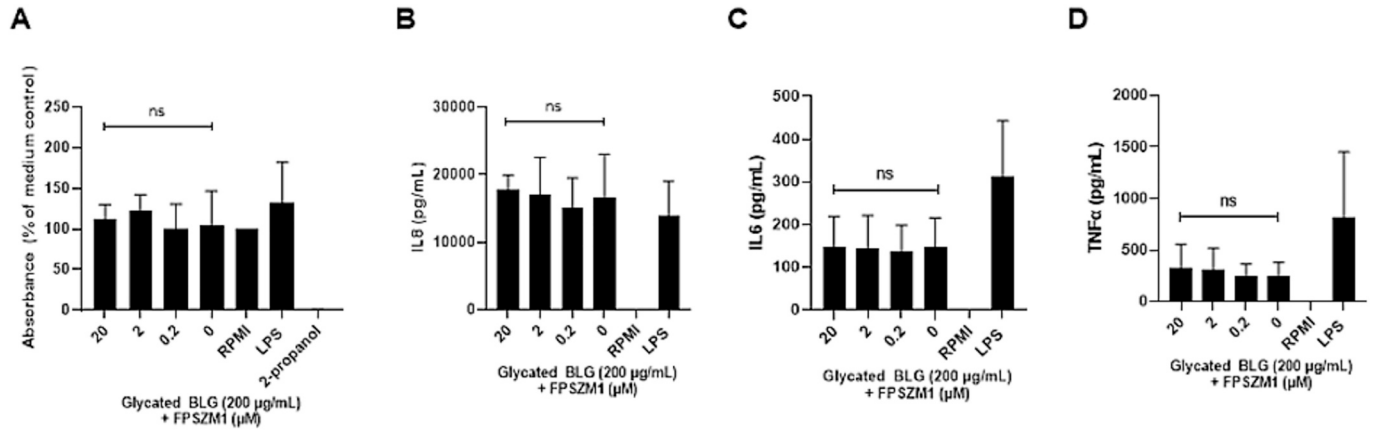

Fig. 7. *Cell viability of M-CSF differentiated M0 macrophages and their IL-8 (B), IL-6 (C) and TNFα (D) secretion upon exposure to glycated beta-lactoglobulin (BLG), after pre-incubation with different concentrations of RAGE inhibitor FPS-ZM1.* BLG was dry heated with glucose for 24 h at 60 °C and 40 % humidity. Subsequently, M-CSF differentiated M0 macrophages were pre-exposed for 1 h to different concentrations of RAGE inhibitor FPS-ZM1 (0-20 µM) before being exposed to this glycated protein for 24 h at 37 °C (5 % CO_2, saturated humidity) at 200 µg/mL. LPS (1 ng/mL) was included as positive control. Data is mean values ± SD obtained from independent experiments performed with three different donors. P-values are obtained by a multiple comparisons test (Tukey) following ANOVA.

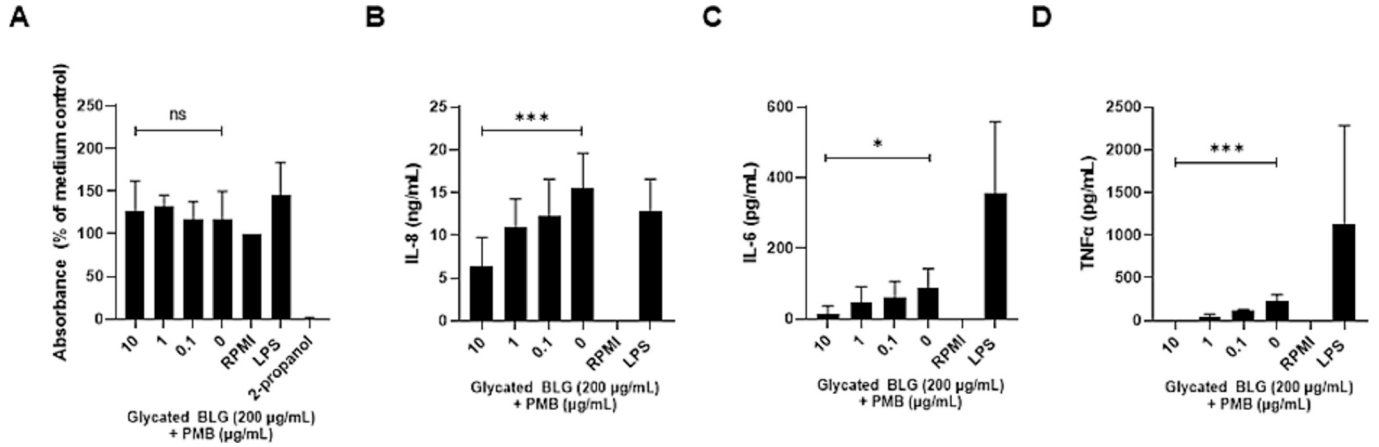

Fig. 8. *Cell viability of M-CSF differentiated M0 macrophages and their IL-8 (B), IL-6 (C) and TNFα (D) secretion upon exposure to glycated beta-lactoglobulin (BLG), co-incubated with different concentrations of polymyxin B (PMB).* BLG was dry heated with glucose for 24 h at 60 °C and 40 % humidity. Subsequently, M-CSF differentiated M0 macrophages were exposed to this glycated protein at 200 µg/mL for 24 h at 37 °C (5 % CO_2, saturated humidity) co-incubated with different concentrations of LPS scavenger PMB (0-10 µg/mL). LPS (1 ng/mL) was included as positive control. Data is mean values ± SD obtained from independent experiments performed with three different donors. P-values (* < 0.05, *** < 0.001) are obtained by a multiple comparisons test (Tukey) following ANOVA.

glycated BLG showing affinity to RAGE according to the competitive sRAGE ELISA (Fig. 5).

2.7. The pro-inflammatory effect of glycated BLG can be inhibited by LPS scavenging

To further explore the inflammatory response of the M-CSF differentiated M0 macrophages induced by the glycated BLG, PMB was added to scavenge potential LPS present in the sample. Supplementary Fig. 2 indicates that PMB did not affect cell viability or act pro-inflammatory at the concentrations used, while Supplementary Fig. 3 shows the strong capacity of PMB to block the pro-inflammatory activity of LPS in our cell model. LPS quantification of the sample showed a level of 0.11 EU/mg protein (=16.5 pg/mg protein), which would normally be considered neglectable, however both M-CSF and GM-CSF differentiated M0 macrophages are sensitive to these levels of LPS and respond to them in a pro-inflammatory fashion as shown in Supplementary Fig. 4. In line with these observations, co-incubation with PMB dose-dependently lowered the pro-inflammatory response induced by glycated BLG in M-CSF differentiated M0 macrophages, as illustrated by the various panels of Fig. 8. For IL-8 and IL-6, a maximal drop of respectively 60 % and 85 % was observed when glycated BLG (200 μg/mL) was co-incubated with 10 μg/mL PMB (resp. $P < 0.001$ and $P < 0.05$)(resp. Fig. 8B and C). In the case of TNFα, the secreted levels dropped below the detection limit at this PMB concentration ($P < 0.001$)(Fig. 8D). Supplementary Fig. 5 shows that the inflammatory response induced by glycated BLG in GM-CSF differentiated M0 macrophages could also be attenuated by PMB. In conclusion, the pro-inflammatory response observed in M0 macrophages was affected by traces of LPS present in the sample.

2.8. Cellular response to commercial glycated proteins varies between manufacturers and batches

In addition to in-house glycated proteins, commercially available glycated proteins were used in many published studies [22,27–32]. Glycated BSA from two different companies (Sigma and Abcam) were characterized and tested on M-CSF differentiated M0 macrophages while being compared to an in-house preparation of glycated BSA. According to the manufacturer information, both preparations were glycated using glycolaldehyde. Data reported in Table 1 depicts that the Sigma preparation showed lower levels of glycation than the Abcam and our in-house preparation. In terms of fluorescence and absorbance, the Sigma sample showed values approximately 2.5-times higher than native BSA, which was used as reference sample. In comparison, the Abcam and our in-house glycated sample showed values 13.5 to 27-times higher, respectively. Looking at the concentration of single Maillard reaction products, the difference in glycation between the Sigma and the other two samples was most profoundly seen in the CEL and CML content. Next to these differences in the level of glycation, a surprising observation was made for the Abcam sample. This preparation showed higher values than the BSA reference for both the lysine and free amino acid content. This would imply that the protein level of this preparation exceeds the 10 mg/mL that is stated in the formulation. The SDS PAGE gel reported in Fig. 9 showed a large amount of high molecular weight structures (>250 kDa) for the Abcam as well as for the Sigma preparation, indicating the presence of big aggregates in these solutions. Interestingly, as shown in Fig. 10, despite these high molecular weight structures, only the in-house preparation showed affinity to sRAGE. When M-CSF differentiated M0 macrophages were exposed to these

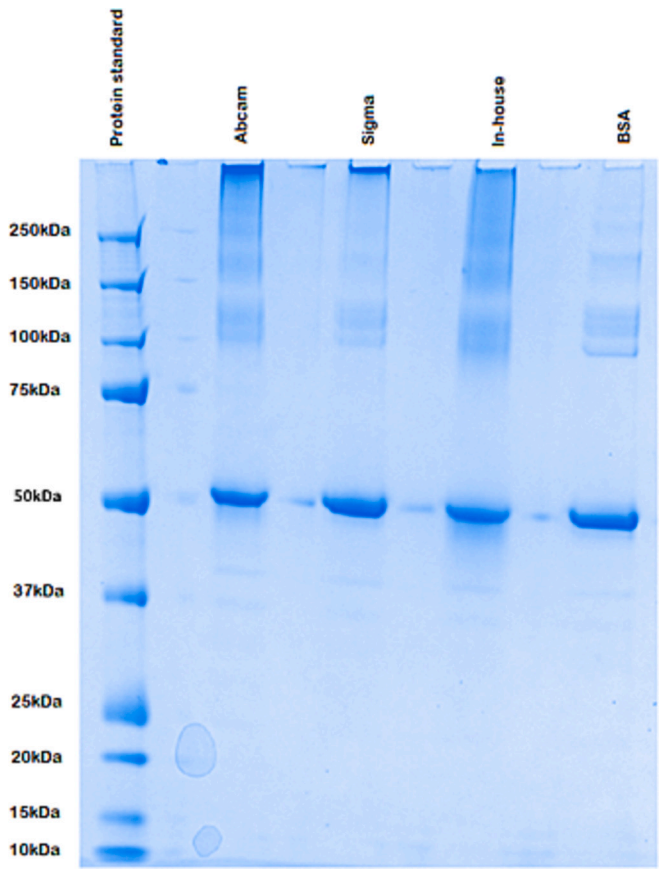

Fig. 9. *SDS-PAGE profile of glycolaldehyde-glycated BSA.* Preparations were purchased from Abcam, Sigma, or made in-house (10 mg/mL BSA in PBS with 10 mM glycolaldehyde for 24 h at 37 °C). Native BSA was included as reference.

Table 1
Fluorescence, absorbance, furosine, CEL, CML, intact lysine, and free amino group content of glycolaldehyde-glycated BSA (10 mg/mL). Preparations were purchased from Abcam, Sigma, or made in-house (10 mg/mL BSA in PBS with 10 mM glycolaldehyde for 24 h at 37 °C). Native BSA was included as reference. Native BSA was included as reference. Fluorescence (in AU) was measured at 370/440 nm, while absorbance (in AU) was measured at 300 nm and corrected for background values at 600 nm. Furosine, CEL, CML and lysine were quantified with LC-MS/MS and expressed as μg/mg protein. Free amino group content were determined with an OPA assay and expressed relative to the BSA solution. Data is mean values ± SD obtained from technical duplicate.

	Fluorescence (370/440 nm)	Absorbance (300-600 nm)	LC-MS/MS (μg/mg protein)				Free amino group content (relative to BSA)
			Furosine	CEL	CML	Intact Lysine	
BSA	91 ± 0.71	0.08 ± 0.01	<DL	<DL	<DL	8.40 ± 0.12	1.0
Sigma	244 ± 0.07	0.22 ± 0.001	0.46 ± 0.004	<DL	1.43 ± 0.08	8.10 ± 0.04	0.9 ± 0.01
Abcam	1631 ± 0.002	2.18 ± 0.05	0.50 ± 0.001	1.27 ± 0.036	4.78 ± 0.01	13.29 ± 0.03	1.4 ± 0.04
In-house	1241 ± 13.67	1.50 ± 0.03	0.49 ± 0.003	0.90 ± 0.003	4.26 ± 0.22	7.43 ± 0.02	0.7 ± 0.02

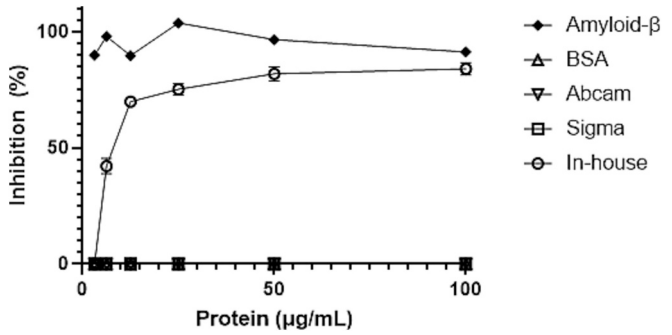

Fig. 10. *Inhibition ELISA for binding of glycolaldehyde-glycated BSA to sRAGE.* Three different preparations were tested: one in-house preparations (10 mg/mL BSA in PBS with 10 mM glycolaldehyde for 24 h at 37 °C) and two commercial preparations from Abcam and Sigma. Aβ-42 was included as positive control, and native BSA as reference. All compounds were tested in duplicate as a two-times dilution series from 100 µg/mL to 3.125 µg/mL. Data is mean values ± SD obtained from a technical duplicate.

preparations, no pro-inflammatory effect was induced as shown by Fig. 11. Interestingly, LPS levels measured in these samples were comparable to the levels measured in the in-house glycated BLG sample discussed before (Supplementary Table 1). All in all, glycolaldehyde-glycated BSA did not act pro-inflammatory in the applied model.

3. Discussion

The objective of this study was to seek a standardized *in vitro* model of dietary AGE-RAGE signaling, to enhance our understanding of the biological activity of glycated dietary proteins. Our data showed that there are three preliminary questions to answer when assessing the inflammatory potential of dietary AGEs *in vitro*:

1) Does the selected cell model express RAGE on the cell surface?
2) Is there solid evidence that LPS is not interfering with the measurements?
3) For both in-house produced and commercially prepared glycated protein samples: are they properly characterized?

3.1. RAGE was only expressed as cell surface receptor in specific in vitro models

According to the AGE-RAGE signaling hypothesis, RAGE is present on the cell surface as a multi-ligand transmembrane receptor. Although all cell lines and primary cells expressed RAGE in our study, it was mainly expressed intracellularly: the receptor was only expressed on the cell surface in marginal amounts, if not absent. We were able to obtain a model that substantially expressed surface RAGE only after differentiating primary monocytes into M0 macrophages with M-CSF. In the literature, many different *in vitro* models have been used to study the inflammatory properties of dietary AGEs. However, the RAGE

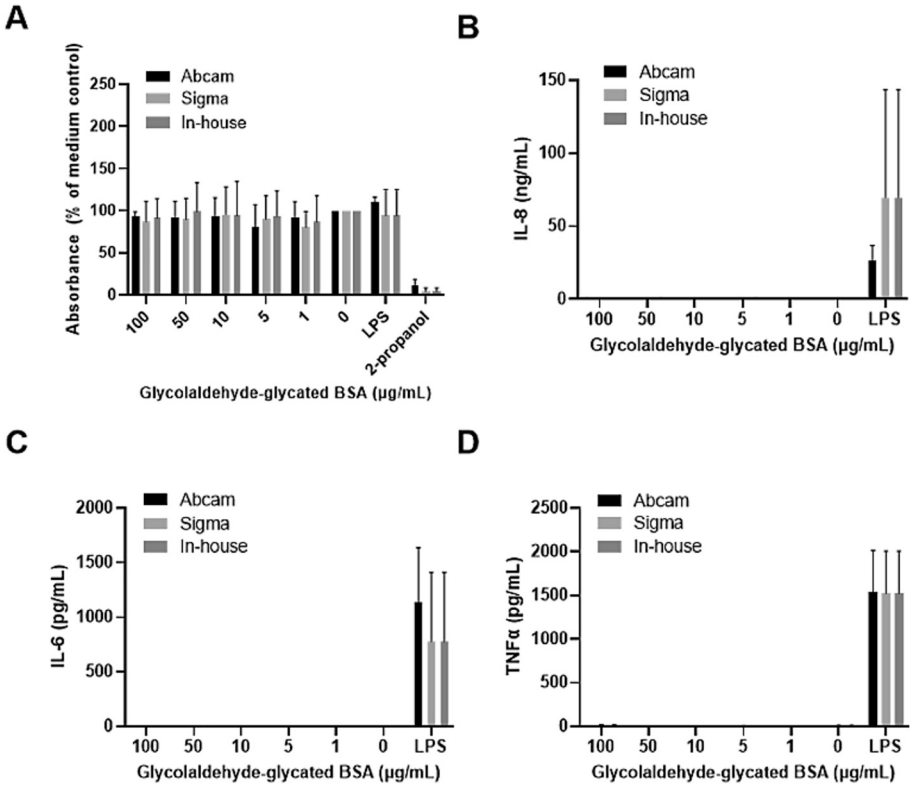

Fig. 11. *Cell viability (A) of M-CSF differentiated M0 macrophages and their IL-8 (B), IL-6 (C) and TNFα (D) secretion upon exposure to different preparations of glycolaldehyde-glycated BSA.* Preparations were purchased from Sigma and Abcam, and an in-house preparation was produced by heating 10 mg/mL BSA in PBS with 10 mM glycolaldehyde for 24 h at 37 °C. M-CSF differentiated M0 macrophages were exposed to these preparations (100-0 µg/mL) for 24 h at 37 °C (5 % CO_2, saturated humidity). LPS (1 ng/mL) was included as positive control. Data is mean values ± SD obtained from independent experiments performed with three different donors. P-values are obtained by a multiple comparisons test (Tukey) following ANOVA.

expression in these models has not been measured [22–24] or only quantified at total RNA (qPCR) or protein (Western-Blot) levels [25,26]. When quantifying RAGE at total RNA or protein level, it is not possible to discriminate between transmembrane and intracellular receptors. Therefore, although positive results for RAGE expression were obtained, the expression of surface RAGE (as suggested in the AGE-RAGE hypothesis) could not be confirmed in these studies. Our data revealed robust total RAGE expression, thereby confirming the results of earlier studies, but showed minimal to no surface RAGE expression in the characterized models. This result underscores the importance of discriminating between both when validating *in vitro* models, as they might exert different physiological functions.

Intracellular RAGE could, for example, play a role in DNA repair. Papers published by Kumar et al. [33,34] describe that nuclear RAGE is part of an early DNA damage response and that deletion of nuclear RAGE leads to persistent double-strand break signaling, leading to senescence, tissue fibrosis, and oncogenesis. Kumar and others suggest nuclear RAGE is a master regulator of double-strand break [35]. Beside this function, it has been suggested that intracellular RAGE is only used for storage and is translocated to the cell surface upon pathological conditions [36]. This hypothesis is in line with the widespread function of RAGE as a multi-ligand transmembrane receptor activating NFκB upon binding to AGEs and other RAGE ligands like Aβ-42. This hypothesis was tested in the current study, however not supported by the data. Possibly, surface RAGE has other, more complex functionalities than inducing an inflammatory response upon single ligand binding.

Our observation that only M-CSF, and not GM-CSF, differentiation-induced surface RAGE expression would suggest a potential anti-inflammatory role for surface RAGE, as M-CSF is used to drive macrophage polarization towards the resolving M2 phenotype while GM-CSF promotes the pro-inflammatory M1 phenotype. The observation of Liliensiek et al. [37] that healthy RAGE knockout mice have a slightly pro-inflammatory phenotype supports our suggestion that RAGE might also be involved in the regulation of anti-inflammatory responses. The Nrf2 signaling pathway, a major mechanism against oxidative stress, might be a target in this respect as Raupbach et al. [25] found pyrraline-modified casein activating this transcription factor in HCT116 cells. More in general, RAGE seems to play a role in the innate rather than the adaptive immune response, as RAGE knockout mice showed lower susceptibility to lethal sepsis while antibody subtypes and the titres did not differ compared to wildtype mice [37]. This reduction in mortality was linked to a decreased number of inflammatory cells adherent to the peritoneum instead of a reduced number of inflammatory cells or cytokine levels in the blood. Chavakis et al. [38] described similar findings, showing impaired leukocyte recruitment to the peritoneum in RAGE knockout mice. They suggested that RAGE interacting with the β2-integrin Mac-1 is required for leukocytes to adhere to the endothelium. Collectively, these data suggest that surface RAGE might play a role in (resolving) innate immune responses, immune cell recruitment, and immune cell tissue adhesion, rather than ligand-induced pro-inflammatory receptor signaling.

Important to note, this study focused on the hypothesis of glycated dietary proteins acting pro-inflammatory through receptor signaling. However, these proteins could also lead to cellular stress through other, RAGE-independent, mechanisms. For example, when specific cell types like macrophages endocytose highly glycated proteins, ubiquitination of these foreign proteins might be hampered due to blockage of the lysine residues by the AGE-modifications. In the absence of ubiquitination, the proteins will not be marked for MHC-I antigen presentation and/or autophagic degradation. At high concentrations, this might lead to the accumulation of aggregates within the cell leading to cellular stress and cell apoptosis [39–41]. Based on the WST-1 results, cell apoptosis in our cell model upon the exposure to the glycated proteins was not observed. However, other glycation methods, longer incubation times and/or higher exposure concentrations might yield different results, so these mechanisms should also be considered when interpreting results in future studies.

3.2. RAGE antagonist could not reduce inflammation induced by glycated dietary proteins, while scavenging LPS reduced inflammation even with negligible LPS levels in the sample

Apart from an alternative function in immune cell recruitment and tissue adhesion, ligand-induced pro-inflammatory signaling by RAGE might also be dependent on the presence of co-stimulatory factors alongside its ligands. In our experiments, LPS scavenging drastically reduced the inflammatory response induced by glycated dietary proteins. In this context, LPS could be a confounding factor or play an active role in RAGE-mediated processes. The former is most straightforward as the RAGE antagonist FPS-ZM1 was not able to attenuate the inflammatory response, suggesting no involvement of surface RAGE in the observed effect. However, although this antagonist has been shown effective before in attenuating inflammatory responses *in vitro* [32,42], its effectiveness for inhibiting RAGE activation in the current cell model could not be confirmed due to lack of a positive control. Therefore the involvement of RAGE in the observed effect cannot be ruled out. Our observation that another frequently described RAGE ligand - Aβ-42 - did also not induce inflammation in our model (Supplementary Fig. 6), despite RAGE affinity being shown by the sRAGE ELISA, reinforces the hypothesis that co-stimulatory factors might be necessary for effective RAGE activation by its described ligands. Since LPS-induced amplification of RAGE-mediated cellular responses has been described before [43,44], the possibility of LPS acting as such a co-stimulatory factor should be considered. To strengthen the conclusions of these studies, using a RAGE knockdown or knockout model would circumvent the possibility of non-effective or cross-reactive antagonists leading to false negative or false positive results, respectively.

Regardless of whether LPS acts as a confounding or co-stimulatory factor, our research stresses the importance of carefully examining it in *in vitro* studies investigating inflammatory processes. Often, *in vitro* studies report their sample being endotoxin free (<1.0 EU/mg protein) according to the manufacturer's or in-house LPS quantification measurements without further consideration. We showed that LPS can still have a significant effect, even though its quantity is below the current safety limits. Interestingly, samples with comparable LPS content did not exhibit the same inflammatory potency. For instance, in the glycated BSA preparations, higher LPS levels seem necessary to induce a pro-inflammatory response. LPS is known to interact with various biomolecules, including proteins, and these interactions can potentially vary depending on the protein of origin or its method of glycation. Such differences may influence the biological activity of LPS or interfere with its accurate quantification [44,45]. Relying solely on an endotoxin-free label or in-house LPS quantification assay to rule out LPS interference might therefore lead to misinterpretation of the results. Since LPS might amplify RAGE-mediated responses, using a LPS scavenger would be more appropriate for detecting LPS interference than a TLR4 inhibitor in this context. Such a scavenger has to be specific for the confounder of interest. In our case, PMB shows high specificity for LPS [46] while, to our knowledge, no data is available suggesting BLG or BSA being retained by PMB. All in all, when investigating the dietary AGE-RAGE signaling hypothesis *in vitro*, LPS interference should be closely monitored to ensure internal validity.

3.3. Characterization of in-house produced and commercially prepared glycated proteins

To compare and combine results from different studies, it is important to have a more in-depth characterization of the glycated dietary proteins tested. A few measures to consider are discussed below. Firstly, LC-MS/MS quantification of AGEs should be performed. This is the validated technique to quantify dietary AGEs and with this technique, databases for the AGE content of different foods have been developed to

easily calculate AGE content in the diet for human observational and intervention studies [16]. Examples of such databases are the Glycation Database of Abertay University [47] and the AGE database of Maastricht University [48]. For *in vitro* studies, glycated proteins are not obtained directly from foods, but food proteins are being glycated in the lab with specific protocols after being isolated and purified. However, AGE quantification of these proteins is often not provided. In this study, the glycated proteins and their controls were characterized for CML, CEL, and Furosine. Next to MG-H1, these dietary AGEs are most frequently analyzed as all of them are (derivatives) of (early-stage) non-crosslinking lysine-derived Maillard reaction products [47]. To obtain a more complete overview, it would be favorable to also quantify cross-linking AGEs like pentosidine, glucosepane, MOLD and GOLD [49]. However, currently these AGEs are not yet often quantified in foods [47]. Regarding this aspect, secondly, the aggregation pattern of the glycated proteins should be visualized with SDS-PAGE or any other adequate technique, since RAGE has been described to only bind AGEs when there are coupled to a relatively large peptide backbone, and high molecular weight structures would facilitate oligomerization of the receptor, which is a process involved in signal transduction [17,18,50]. When combining our SDS-PAGE with sRAGE ELISA results, it seems that the presence of high molecular weight structures alone does not predict the protein's affinity to RAGE, as the presence of high molecular weight structures in the glycated BSA preparations did not necessarily correlate with strong inhibition in the ELISA. For more in-depth understanding of this relationship, characterization of samples with a chemical assay like the sRAGE ELISA is not sufficient. In this case, cell-based assays (*e.g.* fluorescence resonance energy transfer) are preferred, since cellular processes like oligomerization could change the protein's affinity to RAGE [17]. Assessing the glycated protein's affinity to RAGE by a cell-based assay would therefore be our third recommendation for sample characterization in future studies. Lastly, based on our data, it is preferred to study in-house glycated proteins instead of commercial preparations as the purity of the commercial preparations could, in some cases, be questioned. In addition, although using commercially glycated proteins is considered a more standardized and reproducible practice, a full description of commercial glycation methods has not been published and the possibility of significant batch-to-batch variability cannot be excluded. In summary, when studying AGE-RAGE signaling *in vitro,* we suggest to prepare the glycated proteins in-house and subsequently determine its AGE content, aggregation pattern and RAGE affinity with the methods discussed above.

4. Conclusion

In conclusion, our data challenge the existing *in vitro* models used to study the hypothesis on dietary AGE-RAGE signaling. It shows that surface RAGE expression is limited to specific cell conditions and that the inflammatory response induced by the preparation of glycated protein is drastically reduced when LPS is scavenged. This challenges the hypothesis that dietary protein-bound AGEs act pro-inflammatory through RAGE activation. Our data indicates that surface RAGE either has a role beyond facilitating ligand-induced cytokine release or requires a co-stimulatory factor for activation with dietary protein-bound AGEs. Therefore, to better understand the biological activity of dietary AGEs, we recommend future *in vitro* studies to show surface RAGE expression in their model, report thoroughly on glycation methods and glycated protein's characteristics, and closely monitor LPS interference in their experiments. *In vitro* studies lacking these rigorous methodological controls are likely to lead to conclusions that do not fully reflect the physiological relevance of dietary AGEs, thereby hampering the creation of scientific consensus.

5. Experimental procedures

5.1. Materials

All stocks (*e.g.* for M-CSF and GM-CSF) were prepared and stored according to manufacturer instructions. The materials mentioned below are applicable to all protocols unless stated otherwise. From Merck Life Sciences (Darmstadt, Germany), Corning® 96-well microplates (#CLS3595), Corning® T75 cell culture flasks (#CLS430641U), Eppendorf® Safe-Lock 1.5 mL microcentrifuge tubes (#T9661), Dulbecco's Phosphate Buffered Saline (DPBS) without Ca^{2+} and Mg^{2+} (#D857), Bovine Serum Albumin (BSA) (#A3912), Dimethyl sulfoxide (DMSO) (#D2650), and Tween 20 (#P1379) were purchased. RPMI-1640-Glutamax medium (#72400–021), Penicillin-Streptomycin (P/S; 10,000 U/mL) (#15140122) and 0.25 % Trypsin-EDTA (#25200072) were obtained from ThermoFisher Scientific (Waltham, MA, USA). From Sarstedt (Nümbrecht, Germany), 15 mL and 50 mL sterile screw cap tubes (resp. #62.554.502 and #62.547.254) were purchased. From Avantor/VWR (Radnor, PA, USA), Research Grade Foetal Bovine Serum (FBS) (#HYCLSV30160.03; South American Origin) was purchased which was heat inactivated by heating it for 45 min at 56 °C. From Greiner Bio-One (Alphen aan den Rijn, The Netherlands), CELLSTAR 6-well and 12-well microplates (resp. #657160 and #665180) were purchased. UltraPure water was obtained with the Arium 611 VF Water Purifier (Sartorius, Utrecht, The Netherlands).

5.2. Culturing cell lines

Different immortalized cell lines were cultured at 37° C (5 % CO_2 at saturating humidity) in T75 flasks and, for each cell type, $4.0*10^6$ cells were collected to quantify their RAGE expression by flow cytometry.

5.2.1. HMC3

HMC3 microglial cells (#CRL-3304; ATCC, Manassas, VA, USA) were cultured in DMEM, high glucose, GlutaMAX™ with 4.5 g/L D-Glucose and 110 mg/L sodium pyruvate (#10569010; ThermoFisher Scientific, Waltham, MA, USA), supplemented with 10 % non-heat inactivated FBS (#30–2020; ATCC, Manassas, VA, USA) and 1 % P/S. For subculturing, twice a week, cells were trypsinised with 2 mL 0.25 % trypsin-EDTA for 5-10 min at 37 °C until detachment and passaged in a 1:8–1:10 ratio. Passage numbers did not exceed passage 25.

5.2.2. THP-1

Monocytic THP-1 cells (#TIB-202; ATCC, Manassas, VA, USA) were cultured in RPMI-1640-Glutamax, supplemented with 10 % FBS and 1 % P/S. For subculturing, cells were inoculated at $5.0*10^5$ cells/mL twice a week (total volume 12-30 mL) up to passage 25. To differentiate THP-1 monocytes to M0 macrophages, cells were seeded at $1.0*10^6$ cells/mL in a 12-well plate (1 mL/well), with 100 ng/mL PMA (#P1585; Merck Life Sciences, Darmstadt, Germany) supplemented to the medium. At day 2 of culturing, cells were washed twice with pre-warmed medium and fresh medium was added (1 mL/well). After resting for 5 days, cells were collected by incubating with 0.25 % trypsin-EDTA (0.4 ml/well) for 5-10 min at 37 °C until detachment. Immediately thereafter, they were resuspended in culture medium to neutralize the trypsin.

5.2.3. hCMEC/D3

The brain microvascular endothelial cell line hCMEC/D3 (#SCC066; Merck Life Science, Darmstadt, Germany) was cultured in EBM-2 Endothelial Cell Growth Basal Medium-2 (#00190860; Lonza, Basel, Switzerland), supplemented with 5 % FBS (#11560636; ThermoFisher Scientific, Waltham, MA, USA), 1 % P/S, 1 % Chemically Defined Lipid Concentrate (#11905031; ThermoFisher Scientific, Waltham, MA, USA), 10 mM HEPES (#15630080; ThermoFisher Scientific, Waltham, MA, USA), 5 μg/ml L-Ascorbic acid (#A4544; Merck Life Science, Darmstadt, Germany), 1.4 μM Hydrocortisone (#H0888; Merck Life

Science, Darmstadt, Germany), and 1 ng/ml of basic fibroblast growth factor (#GF003; Merck Life Science, Darmstadt, Germany). The cells were grown in flasks precoated with rat tail collagen type I (#08–115; Merck Life Science, Darmstadt, Germany), diluted 1:20 in DPBS. The collagen solution was left for an hour to solidify at 37 °C, and the excess collagen was removed before adding the cells. For subculturing, twice a week, cells were trypsinised with 2 mL 0.25 % trypsin-EDTA for 5-10 min at 37 °C until detachment and passaged in a 1:6 ratio. Passage numbers did not exceed passage 25.

5.2.4. HBVP

The Human Brain Vascular Pericytes cell line HBVP (#P10363-IM; Innoprot, Derio, Spain) were cultured in Pericyte medium (#P600121; Innoprot, Derio, Spain). This medium was purchased as a kit, including FBS, P/S, and pericyte growth supplement, which were all added according to manufacturer's protocol. For subculturing, twice a week, cells were trypsinised with 2 mL 0.05 % trypsin-EDTA (#25300062; ThermoFisher Scientific, Waltham, MA, USA) for 5-10 min at 37 °C until detachment and passaged in a 1:6 ratio. Passage numbers did not exceed passage 25.

5.2.5. Raji

The lymphoblast-like cell line Raji (#CCL-86; ATCC, Manassas, VA, USA) was cultured in RPMI-1640-Glutamax, supplemented with 10 % FBS, 1 % non-essential amino acids (#11140–035; ThermoFisher Scientific, Waltham, MA, USA), and 1 % P/S. For maintenance, half of the medium was refreshed every other day and, up to passage 20, cells were subcultured by inoculating $4.0*10^5$ cells/mL when their density reached $3.0*10^6$ cells/mL (total volume 12-30 mL).

5.2.6. Caco-2

The enterocyte cell line Caco-2 (#CRL-2102; ATCC, Manassas, VA, USA) was cultured with DMEM, high glucose (#10569010; ThermoFisher Scientific, Waltham, MA, USA) supplemented with 10 % FBS, 1 % non-essential amino acids (#11140–035; ThermoFisher Scientific, Waltham, MA, USA), and 1 % P/S. For subculturing, twice a week, cells were trypsinised with 2 mL 0.25 % trypsin-EDTA for 5-10 min at 37 °C until detachment and passaged in a 1:3–1:6 ratio. Cells were used between passage 45 and 55.

5.3. Monocyte isolation

Per donor, 50 mL buffycoat (#B2825R00; Sanquin, Nijmegen, The Netherlands) was mixed with 50 mL 2 % FBS-DPBS (with Ca^{2+} and Mg^{2+}; #14040–091; ThermoFisher, Waltham, MA, USA), and equally divided over four 50 mL Leucosep tubes (#227290; Greiner Bio-One, Alphen aan den Rijn, The Netherlands). These Leucosep tubes were pre-treated with Ficoll® Reagent (#GE17–1440-03; Merck Life Sciences, Darmstadt, Germany), by adding 15 mL of this reagent to the tube and spinning it at room temperature (RT) for 30s at 1000*g. The tubes containing buffycoat were centrifuged at 4 °C, first for 5 min at 200*g followed by 15 min at 500*g (slow brake). Subsequently, the upper plasma layer was removed and the cells were collected and washed by adding 2 % FBS-DPBS and centrifuging at RT for 10 min at 300*g (slow brake). After repeating the washing step, the cell pellet was resuspended in 2 mL of MACS buffer (2 % FBS-DPBS (without Ca^{2+} and Mg^{2+}) with 2 mM EDTA (#E6758; Merck Life Sciences, Darmstadt, Germany)). To isolate monocytes, CD14 microbeads (#130–050-201; Miltenyi Biotec, Bergisch Gladbach, Germany) were added according to the manufacturer's protocol. After 15 min incubation at 4 °C, 10 mL MACS buffer was added and the suspension was centrifuged at 4 °C for 10 min at 300*g (slow brake). The cell pellet was resuspended in 500 μl MACS buffer and loaded onto a LS column with 30 μm pre-separation filter (#130–041-407; Miltenyi Biotec, Bergisch Gladbach, Germany) placed in a QuadroMACS™ separator (#130–090-976; Miltenyi Biotec, Bergisch Gladbach, Germany). The column was washed three times with 3 mL MACS buffer. Then, the column was removed from the MACS separator. MACS buffer (5 mL) was applied to the column and the magnetically labelled cells were immediately flushed out by firmly pushing a plunger into the column. After determining the cell concentration using the Corning® Cell Counter (#734–3259; Avantor/VWR, Radnor, PA, USA), the suspension was centrifuged at 4 °C for 10 min at 300*g (slow brake). Until further use, these cells were stored in liquid nitrogen in FBS/10 % DMSO.

5.4. Differentiation of monocyte to M0 macrophages

For cell culture, primary monocytes from liquid nitrogen were thawed at 37 °C and the content was transferred to pre-warmed 9 mL RPMI-1640-Glutamax supplemented with 20 % FBS and 1 % P/S. The suspension was centrifuged at RT for 8 min at 300*g. The pellet was resuspended in culture medium (RPMI-1640-Glutamax supplemented with 10 % FBS and 1 % P/S). Next, for flow cytometry analysis of monocytes, cells were seeded at $5.0*10^5$ cells/mL in a 6-well plate (8 mL/well). After overnight resting (37 °C, 5 % CO_2 at saturating humidity), the monocytes were collected in a 15 mL tube by resuspending and scraping, and flow cytometry protocol was followed. For flow cytometry analysis of M0 macrophages, M-CSF or GM-CSF (resp. #216-MCC and #7954-GM; Bio-Techne, Minneapolis, MN, USA) was added to the culture medium to a final concentration of 50 ng/mL. Instead of overnight resting, cells were cultured for 7 days and, at day 3 and 5 of culturing, medium was refreshed containing new 50 ng/mL M-CSF or GM-CSF. At day 7, M0 cells were trypsinised with 0.25 % trypsin-EDTA (2 ml/well) for 10 min (37 °C, 5 % CO_2 at saturating humidity) and collected by scraping. Immediately thereafter, they were resuspended in culture medium to neutralize the trypsin. Subsequently, the flow cytometry protocol was followed. To test the effects of glycated proteins on M0 macrophages, a similar culture protocol was followed, however cells were seeded in a 96-well culture plate (200 μL/well). At day 7, supernatant was removed, whereafter experimental conditions were added (100 μL/well) and incubated for 24 h (37 °C, 5 % CO_2 at saturating humidity).

5.5. Flow cytometry protocol for RAGE detection

In order to detect RAGE, cells were centrifuged at RT for 3 min at 300*g after collection. The pellet was resuspended in 4 mL DPBS and this cell suspension was divided over four 1.5 mL Eppendorf tubes, corresponding to an initial cell count of $1.0*10^6$ cells/Eppendorf. The centrifugation step was repeated and cells were stained with or without being fixed and permeabilized first. In case of fixation-and-permeabilization being applied, which was the case for half of the tubes, each pellet was reconstituted in 100 μL of fixation buffer (2 % formaldehyde in DPBS) (made from Pierce™ 16 % Formaldehyde (w/v); #28908; ThermoFisher Scientific, Waltham, MA, USA). After 15 min incubation at RT, cells were washed by adding 1 mL DPBS and centrifuging similar to previous steps. Each cell pellet was thereafter reconstituted in 100 μL permeabilization buffer (1 % BSA-DPBS with 0.1 % saponin) (#47036; Merck Life Sciences, Darmstadt, Germany). After 15 min incubation at RT, the cells were washed once more to finalize the fixation and permeabilization. Subsequently, all samples were reconstituted in 10 μL FcR Blocking Reagent (#130–059-901; Miltenyi Biotec, Bergisch Gladbach, Germany) and incubated for 10 min at 4 °C in the dark. Afterwards, 90 μL RAGE polyclonal antibody (1:50 dilution in DPBS; validated for the epitope being on the V-domain of RAGE) (#PA5–24787; ThermoFisher, Waltham, MA, USA) was added a permeabilized and a non-permeabilized sample. To the other two samples, 90 μL DPBS was added which served as negative control to help differentiate non-specific background signal from specific antibody signal. Samples were incubated for 30 min at 4 °C in the dark. After washing, all samples were reconstituted in 100 μL Alexa Fluor 647 Goat Anti-Rabbit IgG recombinant antibody (1:200 dilution in DPBS) (#A27040;

ThermoFisher, Waltham, MA, USA). After incubating for 30 min at 4 °C in the dark, cells were washed and reconstituted in 100 μL DPBS to be analyzed on the CytoFLEX Flow Cytometer (Beckman Coulter, Fullerton, CA, USA). For each sample, 10.000 cells were measured at a speed of 10 μL/min. Data was analyzed in CytExpert Software (Beckman Coulter, Fullerton, CA, USA). First, debris was excluded based on SSC-A *vs* FSC-A gating, whereafter doublets were excluded by FSC-H *vs* FSC-A and SSC-H *vs* SSC-A gating. Based on this gating strategy, percentage of positive cells and median fluorescent intensity (MFI) (APC channel) were determined. The former parameter is defined as the percentage of positive cells in the sample of interest relative to 1 % positive cells in the corresponding negative control sample (stained without primary antibody), whereas the latter is defined as the MFI of the sample of interest corrected by subtraction for the MFI of the corresponding negative control sample.

5.6. Protein glycation

Beta-Lactoglobulin (BLG) (#L0130; Merck Life Sciences, Darmstadt, Germany) was dissolved to 10 mg/mL in DPBS with or without 16 mM D-glucose (#G7021; Merck Life Sciences, Darmstadt, Germany). These solutions were lyophilized in aliquots of 500 μL in 5.0 mL Sterile Eppendorf® tubes (#525–0982; Avantor/VWR, Radnor, PA, USA). Apart from the native protein control, these lyophilized aliquots were heated in a Memmert Environmental Chamber (#10861–384; Avantor/VWR, Radnor, PA, USA) at 60 °C and 40 % humidity for 9 h, 12 h, and 24 h, to approach temperatures reached during food processing without denaturating BLG. Afterwards, they were redissolved in 500 μL DPBS. Glycated BSA samples were purchased from Sigma (#121800-M) and Abcam (#Ab51995), or prepared in-house. BSA (#A7030; Merck Life Sciences, Darmstadt, Germany) was dissolved to 10 mg/mL in DPBS with 10 mM glycolaldehyde (#G6805; Merck Life Sciences, Darmstadt, Germany). 1 mL aliquots were heated in 1.5 mL Eppendorf tubes in a heating block at 37 °C for 24 h. Residual glucose and glycolaldehyde were removed by 10 kDa MWCO, Amicon™ Filter (#UFC9010; Merck Life Sciences, Darmstadt, Germany) according to manufacturer protocol. For each sample, final protein concentration was determined by DUMAS, to be able to account for potential losses. The conversion factor of 6.38 was applied. Samples were stored at −20 °C.

5.7. Characterization

Glycated samples and their controls were characterized in terms of absorbance, fluorescence, AGE levels, free amino group content, LPS levels, aggregation pattern and sRAGE binding capacity.

5.7.1. Absorbance and fluorescence

Samples (10 mg/mL) were analyzed in duplicate for absorbance and fluorescence in resp. transparent and black 96-well plates (100 μL/well). Fluorescence was measured at λexc 370 nm and λem 440 nm, while absorbance was measured at 300 and 600 nm using a Spectramax® M2.

5.7.2. Free amino group content by OPA

To perform an Phthaldialdehyde (OPA) assay, OPA solution was made by dissolving 3.81 g sodium tetraborate (#1.06308; Merck Life Sciences, Darmstadt, Germany), 88 mg dithiothreitol (#D0632; Merck Life Sciences, Darmstadt, Germany), and 100 mg sodium dodecyl sulphate (#8.22050; Merck Life Sciences, Darmstadt, Germany) in 97 mL UltraPure water at 35–40 °C, and subsequently adding a 3 mL ethanol mixture of 80 mg OPA (#1.11452; Merck Life Sciences, Darmstadt, Germany). The OPA solution was kept in the dark and used within 2 h. For the analysis, 10 μL of the glycated samples (10 mg/mL) together with 200 μL of the OPA solution were added to a transparent 96-well plate. For the blank, 10 μL UltraPure water was added to the OPA solution. The plate was incubated for 15 min at RT in the dark, and absorbance was measured at 340 nm. All analysis were performed in duplicate and free amino group content was determined using a six-point two-times serial dilution curve of L-Leucine (2000 μg/mL) (#L8000; Merck Life Sciences, Darmstadt, Germany) and presented relative to the free amino group content of the untreated (native) sample.

5.7.3. AGE levels (intact Lysine, CML, CEL and furosine) by LC-MS/MS

Protein samples were diluted to 8 mg/mL in DPBS and 50 μL was added to 1 mL 6 M HCl in a glass heating tube. The headspace of these tubes was saturated with nitrogen before closing them off with a cap. Tubes were heated at 110 °C on a heating block for 22 h. After heating, 400 μL was transferred to a MS vial (#AR0–3921-13; Phenomenex, Woerden, The Netherlands) and dried with a vacuum concentrator (#RVC 2–33 CDplus; CHRIST, Osterode am Harz, Germany) set at 4.5 mbar (2 h, 30 °C). Samples were reconstituted in 500 μL UltraPure water and purified by solid phase extraction. In this respect, Oasis HLB 1 cc cartridges (#WAT094225; Waters, Etten-Leur, The Netherlands) were activated by loading and running 1 mL methanol (#0013684101BS; Biosolve, Valkenswaard, The Netherlands) succeeded by 1 mL 10 mM nonafluoropentanoic acid (NFPA) (#396575; Merck Life Sciences, Darmstadt, Germany) in Ultrapure water, before loading the samples. Thereafter, the columns were washed with 1 mL 10 mM NFPA/MeOH (95:5, *v*/v) and analytes were eluted by running 1 mL 10 mM NFPA/MeOH (1:1, v/v). These eluents were dried in MS vials with a vacuum concentrator set at 4.5 mbar (2 h, 30 °C) and reconstituted in 200uL ultrapure water/acetonitrile (#0001204101BS; Biosolve, Valkenswaard, The Netherlands) (1:1, v/v) containing an internal standard mixture (0.5 ppm) consisting of L-Lysine-4,4,5,5-d4 hydrochloride (#616192; Merck Life Sciences, Darmstadt, Germany), CML-d4 (#HAA2952; Iris Biotech, Marktredwitz, Germany), CEL-d4 (#HAA2941; Iris Biotech, Marktredwitz, Germany), and Furosine-d4 (#HAA2961; Iris Biotech, Marktredwitz, Germany). The calibration curve for the analysis was a 12-point 3-times serial dilution (2 ppm-11.3 ppt) of L-Lysine hydrochloride (#4400-M; Merck Life Sciences, Darmstadt, Germany), CML (#HAA2950; Iris Biotech, Marktredwitz, Germany), CEL (#HAA2940; Iris Biotech, Marktredwitz, Germany), and Furosine (#HAA2960; Iris Biotech, Marktredwitz, Germany) in ultrapure water/acetonitrile (1:1, v/v) containing the abovementioned internal standard mixture (0.5 ppm). All samples and calibration solutions were stored at −20 °C for maximal one week before LC-MS/MS analysis.

Sample analysis was carried with a Nexera UPLC system (Shimadzu Corporation, Kyoto, Japan) coupled with a LCMS-8050 triple quadrupole mass spectrometer (Shimadzu Corporation, Kyoto, Japan). The UPLC unit consisted of a SIL-30AC autosampler, a LC-20ADXR solvent delivery module, DGU-20ASR degassing unit, a CTO-20AC column oven and a FCV-20AH2 valve unit. The samples (5 μL) were injected on a Kinetex HILIC 2.6 μm, 2.1 mm × 100 mm (Phenomenex B.V., Torrance, CA, USA). The flow rate was set at 0.4 mL/min and the column temperature at 30 °C. The mobile phases consisted of 0.1 % formic acid (solvent A), acetonitrile with 0.1 % formic acid (solvent B) and 50 mmol/L ammonium formate (solvent C) with the following elution profile (t in [min]/[%B]/[%C]): (0/80/10), (0.8/80/10), (3.5/40/10), (6.5/40/10), (8.0/80/10) and (10.0/80/10). MS data was collected for 10 min. Positive ionization mode was used for all MS analyses. The voltage of the turbo ion-spray ionization was 4.0 kV. The temperature of the electrospray ionization probe, desolvation line, and heat block were set at 300 °C, 250 °C, and 400 °C, respectively. The pressure of the collision-induced dissociation gas was 4 kPa whereas the flow rates of the drying gas, nebulizer gas, and heating gas were set at 10 mL/min, 3 mL/min, and 10 mL/min, respectively. The electrode voltage of Q1 pre bias (collision cell energy entrance potential), collision cell Q2 (collision energy), Q3 pre bias (collision cell energy exit potential), parent and fragment ion *m/z* of the multiple reaction monitoring transitions were optimized using the support software (LabSolutions, Shimadzu Corporation, Kyoto, Japan). For single reaction monitoring (SRM), the dwell time was set at 32 msec and the most abundant fragment ion was

selected for quantitation. The second and third fragments in ion yield were selected as structural confirmation based on the optimized SRM transition (Supplementary Table 2).

Analytical data was processed with LabSolutions software (Shimadzu Corporation, Kyoto, Japan). For all samples and calibration solutions, the integrated peak area of each analyte was divided by the corresponding integrated peak area of the deuterated standard to correct for matrix effects. Analyte content in the samples was quantified by interpolating these corrected integrated peak area from the calibration curve. The limit of detection was defined as the concentration corresponding to the smallest corrected integrated peak area included in the calibration curve (based on the deviation of the slope), which was 0.3 ppb for all analytes corresponding to 0.4 ng/mg protein. Analyte contents are presented as per the amount of protein. As a quality control measure, an additional native BLG sample was spiked with the internal standards (0.5 ppm) prior to SPE and recovery values were calculated: $\frac{\text{measured concentration–theoretical concentration}}{\text{theoretical concentration}}*100\%$. For all analytes, this values was within the acceptable limit of ±20 %.

5.7.4. LPS levels by LAL assay

LPS concentrations were determined for the glycated proteins tested in cell culture experiments, using the Pierce LAL Chromogenic Endotoxin Quantitation Kit (A39552; ThermoFisher, Waltham, MA, USA). The test kit was used according to the manufacturer's instructions. To ensure a sterile environment devoid of lipopolysaccharides, LPS-free water, pipette tips, and tubes were employed for the experiment. Additionally, the spatulas were washed with 1 M NaOH before weighing any compounds to mitigate the risk of LPS contamination.

5.7.5. Aggregation pattern by SDS page

6uL of NuPAGE™ LDS sample buffer (#NP0007; ThermoFisher, Waltham, MA, USA) was added to 1 μg protein and brought to a final volume of 24 μL with deionized water. This mixture was heated for 10 min at 70 °C and afterwards, samples were loaded on a NuPAGE™ 12 % BisTris 1.0 mm 10-well Gel (#NP0341, ThermoFisher Scientific, Waltham, MA, USA) (18uL/well; 1.5 μg protein/well). As a reference, 5 μL of a prestained protein standard (#1610377; Bio-Rad, Hercules, CA, USA) was loaded. This gel was run with NuPAGE™ MOPS Running Buffer (#NP0001; ThermoFisher, Waltham, MA, USA) at 120 V in a XCell SureLock™ Mini-Cell (#EI0001; ThermoFisher Scientific, Waltham, MA, USA) until, after approximately 90 min, the dye front reached the bottom of the gel. The gel was washed with deionized water 4 times for 5 min to remove SDS present in the gel before covering the gel with PageBlue™ Protein Staining Solution (#24620; ThermoFisher Scientific, Waltham, MA, USA) and staining it for 1 h at RT on a shaker. Then, the gel was washed with deionized water 2 times for 5 min before washing it in overnight in deionized water. After overnight washing, gel was put on a white light conversion screen (#1708289; Bio-Rad, Hercules, CA, USA) and picture was taken with ChemiDoc MP machine (Bio-Rad, Hercules, CA, USA) using the Coomassie Blue staining setting.

5.7.6. sRAGE binding capacity by sRAGE ELISA

A Nunc™ Maxisorp™ 96 well plate (#44–2404; ThermoFisher, Waltham, MA, USA) was coated with 40 μg/mL glycated soy extract [51] in 1.5 mM sodium carbonate buffer (6.8 g/L Na_2CO_3 and 11.4 g/L $NaHCO_3$ in UltraPure water, pH 9.6), 80 μL/well, and incubated overnight at 4 °C in the dark. Next, the plate was washed three times with 0.05 % (*v*/v) Tween 20-PBS (0.24 g/L KH_2PO_4, 1.78 g/L $Na_2HPO_4{\cdot}2H_2O$, 0.2 g/L KCL, and 8 g/L NaCl in UltraPure Water, pH 7.4), 200 μL/well, and incubated with 3 % BSA-PBS (#BSAV-RO (Fraction V); Merck Life Sciences, Darmstadt, Germany), 150 μL/well, for 1 h at RT. Meanwhile, protein samples and amyloid beta 1–42 (Aβ-42) (#HB9805; Hello Bio, Dunshaughlin, Ireland) were 2-times serial diluted (100–3.125 μg/mL) in dilution buffer (1.5 % BSA-PBS with 0.0125 % Tween 20) with 0.5 μg/mL sRAGE (#RD172116100; BioVendor R&D, Brno, Czech Republic) in a 450 μL Nunc™ Polystyrene dilution plate (200 μL/well final volume) (#267245; ThermoFisher Scientific, Waltham, MA, USA) and incubated for 45 min at 37 °C on a shaker. In addition to the protein samples, dilution buffer with and without 0.5 μg/mL sRAGE were included as controls. After incubation, the Maxisorp plate was washed three times, and samples plus controls from the dilution plate were added in duplicate to this Maxisorp plate (80 μL/well). After 1 h incubation at 37 °C on a shaker, the plate was washed five times before adding 80 μL/well primary RAGE antibody (#MAB11451; Bio-Techne, Minneapolis, MN, USA) (0.5 μg/mL in dilution buffer). Plate was incubated for 30 min at RT on a shaker and afterwards washed 5 times before adding 80 μL/well Goat Anti-Mouse antibody-HRP (P0447; Agilent, Santa Clara, CA, USA) (1:1000 in dilution buffer). Plate was incubated for 30 min at RT on a shaker and then washed 4 times before adding 80 μL/well TMB solution (#T4444; Merck Life Sciences, Darmstadt, Germany). After 10 min incubation at RT in the dark, 100 μL/well 2 M H_2SO_4 was added. Absorbance was measured at 450 and 540 nm with Spectramax® M2. For the data analysis, OD values of 540 nm were subtracted from OD values of 450 nm and these OD values were averaged for each duplicate. Percentage of Inhibition, as a measure for RAGE binding affinity, was calculated by applying the following formula: $\frac{ODdilution\ buffer\ with\ sRAGE-(ODsample-ODdilution\ buffer\ without\ sRAGE)}{ODdilution\ buffer\ with\ sRAGE}*100\%$. The limit of quantification was considered 25 %.

5.8. Cell culture experiments

To test the inflammatory properties of glycated proteins, M0 macrophages were exposed to a concentration range of 24 h glucose-glycated BLG (1000, 100, 10, and 1 μg/mL) and glycolaldehyde-glycated BSA (100, 50, 10, 5, and 1 μg/mL). These preparations were either produced in-house or purchased, as described in the section 'Protein Glycation'. Culture medium and 1 ng/mL LPS (#L3137; Merck Life Sciences, Darmstadt, Germany) served as negative and positive controls, respectively. When preparations showed a pro-inflammatory response, the cells were pre-incubated with different concentrations of FPSZM1 (#6237; Bio-Techne, Minneapolis, MN, USA) (20, 2, 0.2 μM) for 1 h before adding glycated BLG or BSA (resp. 200 and 10 μg/mL). In addition, glycated BLG and BSA were *co*-incubated with different concentrations of Polymyxin B (PMB) (10, 1, 0.1 μg/mL) (#P4932; Merck Life Sciences, Darmstadt, Germany). In all cases, after 24 h of exposure, a WST-1 assay was performed on the cells and the supernatant was collected and stored at −20 °C for further cytokine analysis.

5.8.1. WST-1 assay

Cell proliferation was determined using a WST-1 assay. Briefly, 110 μL/well WST-1 mixture was added to the cells. This mixture consisted of WST-1 reagent (#CELLPRO-RO; Merck Life Sciences, Darmstadt, Germany) added to the culture medium (final dilution 1:10). As a positive control, cells were pre-exposed for 10 s to 10 μL 70 % 2-propanol (#8167045000; Actu-All Chemicals, Oss, The Netherlands). Cells were incubated with the mixture for 90 min at 37 °C (5 % CO2 at saturating humidity), before absorbance was measured at 450 and 540 nm with a Spectramax® M2 (Molecular Devices, San Jose, CA, USA). For data analysis, these OD values at 450 nm were corrected for those at 540 nm. Corrected OD values of duplicate measurements were averaged and expressed as percentage of the negative control (culture medium).

5.8.2. Cytokine ELISA

IL-8, IL-6 and TNF-α levels were quantified with Human Duoset ELISA kits (resp. #DY208, #DY206 and #DY210; Bio-Techne, Minneapolis, MN, USA). Manufacturer protocol was followed, however TMB substrate, supersensitive, for ELISA (#T4444; Merck Life Sciences, Darmstadt, Germany) was used as substrate solution. Absorbance was measured at 450 nm and 540 nm using a Spectramax® M2. For data

analysis, the OD values (450-540 nm) of technical duplicates were averaged and corrected for the blank. Sample concentrations were determined by interpolating these OD values against the standard curve by GraphPad Prism 9 (GraphPad Software, La Jolla, CA) and correcting them for the dilution factor. For samples with an average OD value below the LLOQ, the concentration was considered zero.

5.8.3. Statistics

All cell culture experiments were repeated at least 3 times ($n = 3$). Results are stated as mean ± SD from these independent experiments, unless stated otherwise. One-way analysis of variance (ANOVA) followed by Tukey's multiple comparison test was used for statistical analysis in IBM SPSS statistics 25 (SPSS Inc., Chicago, IL, USA). A p-value of ≤ 0.05 was considered statistically significant. All graphs were created using GraphPad Prism 9 (GraphPad Software, La Jolla, CA).

CRediT authorship contribution statement

Fleur A.C. Jansen: Writing – original draft, Methodology, Investigation, Conceptualization. **Josep Rubert:** Writing – review & editing, Supervision. **Klaske van Norren:** Writing – review & editing, Supervision. **Vincenzo Fogliano:** Writing – review & editing, Supervision, Conceptualization. **Tamara Hoppenbrouwers:** Writing – review & editing, Supervision, Methodology.

Funding information

This research did not receive any specific grant from funding agencies in the public, commercial, or not-for-profit sectors.

Declaration of competing interest

The authors declare that they have no known competing financial interests or personal relationships that could have appeared to influence the work reported in this paper.

Acknowledgements

The authors would like to express their gratitude to Marialena Chrysanthou for the fruitful discussions on the topic.

Appendix A. Supplementary data

Supplementary data to this article can be found online at https://doi.org/10.1016/j.ijbiomac.2025.144889.

References

[1] P. Ulrich, A. Cerami, Protein Glycation, Diabetes, and Aging, 2001.
[2] N. Verzijl, J. Degroot, E. Oldehinkel, R.A. Bank, S.R. Thorpe, J.W. Baynes, et al., Age-related accumulation of Maillard reaction products in human articular cartilage collagen, Biochem. J. 350 (2000).
[3] M. Smuda, C. Henning, C.T. Raghavan, K. Johar, A.R. Vasavada, R.H. Nagaraj, et al., Comprehensive analysis of maillard protein modifications in human lenses: effect of age and cataract, Biochemistry 54 (15) (2015) 2500–2507, https://doi.org/10.1021/bi5013194.
[4] V.M. Monnier, R.R. Kohn, A. Cerami, Accelerated age-related browning of human collagen in diabetes mellitus, Proc. Natl. Acad. Sci. USA 81 (2) (1984) 583–587, https://doi.org/10.1073/PNAS.81.2.583.
[5] R. Ramasamy, S.J. Vannucci, S.S. Yan, Du, K. Herold, S.F. Yan, A.M. Schmidt, Advanced glycation end products and RAGE: a common thread in aging, diabetes, neurodegeneration, and inflammation, Glycobiology (2005), https://doi.org/10.1093/glycob/cwi053.
[6] C. Ott, K. Jacobs, E. Haucke, A. Navarrete Santos, T. Grune, A. Simm, Role of advanced glycation end products in cellular signaling, Redox Biol. 2 (1) (2014) 411–429, https://doi.org/10.1016/J.REDOX.2013.12.016.
[7] L.J. Sparvero, D. Asafu-Adjei, R. Kang, D. Tang, N. Amin, J. Im, et al., RAGE (receptor for advanced glycation endproducts), RAGE ligands, and their role in cancer and inflammation, J. Transl. Med. (2009), https://doi.org/10.1186/1479-5876-7-17.
[8] A.M. Schmidt, Isolation and characterization of two binding proteins for advanced glycosylation end products from bovine lung which are present on the endothelial cell surface, J. Biol. Chem. 267 (21) (1992) 14987–14997, https://doi.org/10.1016/S0021-9258(18)42137-0.
[9] M. Neeper, A. Marie Schmidt, J. Brett, S. Du YanQ, F. Wangll, Y.-C.E. Pan, et al., Cloning and expression of a cell surface receptor for advanced glycosylation end products of proteins, J. Biol. Chem. 267 (21) (1992) 14998–15004.
[10] D.M. Stern, S.Du. Yan, S.F. Yan, A.M. Schmidt, Receptor for advanced glycation endproducts (RAGE) and the complications of diabetes, Ageing Res. Rev. 1 (2002) 15.
[11] M. Snelson, E. Lucut, M.T. Coughlan, The role of AGE-RAGE signalling as a modulator of gut permeability in diabetes, Int. J. Mol. Sci. 23 (3) (2022).
[12] L. Lin, S. Park, E.G. Lakatta, RAGE signaling in inflammation and arterial aging, 2009.
[13] K. Kierdorf, G. Fritz, RAGE regulation and signaling in inflammation and beyond, J. Leukoc. Biol. 94 (1) (2013) 55–68, https://doi.org/10.1189/jlb.1012519.
[14] A.M.A. Linkens, N. van Best, P.M. Niessen, N.E.G. Wijckmans, E.E.C. de Goei, J.L.J. M. Scheijen, et al., A 4-week diet low or high in advanced glycation Endproducts has limited impact on gut microbial composition in abdominally obese individuals: the deAGEing trial, Int. J. Mol. Sci. 23 (10) (2022) 5328, https://doi.org/10.3390/IJMS23105328.
[15] A.M.A. Linkens, A.J.H.M. Houben, P.M. Niessen, N.E.G. Wijckmans, E.E.C. de Goei, M.D.G. Van den Eynde, et al., A 4-week high-AGE diet does not impair glucose metabolism and vascular function in obese individuals, JCI Insight 7 (6) (2022), https://doi.org/10.1172/JCI.INSIGHT.156950.
[16] C. Delgado-Andrade, V. Fogliano, Dietary advanced glycosylation end-products (dAGEs) and Melanoidins formed through the Maillard reaction: physiological consequences of their intake, Annu. Rev. Food Sci. Technol. 9 (2018) 271–291, https://doi.org/10.1146/ANNUREV-FOOD-030117-012441.
[17] J. Xie, S. Reverdatto, A. Frolov, R. Hoffmann, D.S. Burz, A. Shekhtman, Structural basis for pattern recognition by the receptor for advanced glycation end products (RAGE), J. Biol. Chem. 283 (40) (2008) 27255–27269, https://doi.org/10.1074/JBC.M801622200.
[18] J. Xue, V. Rai, D. Singer, S. Chabierski, J. Xie, S. Reverdatto, et al., Advanced glycation end product recognition by the receptor for AGEs, Structure 19 (5) (2011) 722–732, https://doi.org/10.1016/j.str.2011.02.013.
[19] D. Zhao, B. Sheng, Y. Wu, H. Li, D. Xu, Y. Nian, et al., Comparison of free and bound advanced glycation end products in food: a review on the possible influence on human health, J. Agric. Food Chem. 67 (51) (2019) 14007–14018, https://doi.org/10.1021/acs.jafc.9b05891.
[20] C. Dubois, R. Litke, S. Rianha, C. Paul-constant, J.M. Lo Guidice, S. Taront, et al., Exposure of *caenorhabditis elegans* to dietary nε-carboxymethyllysine emphasizes endocytosis as a new route for intestinal absorption of advanced glycation end products, Nutrients 13 (12) (2021), https://doi.org/10.3390/nu13124398.
[21] Y. Wu, M. Zong, Z. Zhang, Y. Wu, L. Li, X. Zhang, et al., Selective transportation and energy homeostasis regulation of dietary advanced glycation end-products in human intestinal Caco-2 cells, Food Chem. 391 (2022) 133284, https://doi.org/10.1016/J.FOODCHEM.2022.133284.
[22] L. Paparo, S. Coppola, R. Nocerino, L. Pisapia, G. Picariello, M. Cortese, et al., How dietary advanced glycation end products could facilitate the occurrence of food allergy, J. Allergy Clin. Immunol. 153 (3) (2024) 742–758, https://doi.org/10.1016/j.jaci.2023.11.023.
[23] T. Van Der Lugt, A.R. Weseler, W.A. Gebbink, M.F. Vrolijk, A. Opperhuizen, A. Bast, Dietary advanced glycation endproducts induce an inflammatory response in human macrophages in vitro, Nutrients 10 (12) (2018), https://doi.org/10.3390/nu10121868.
[24] T. Toyomura, M. Watanabe, H. Wake, T. Nishinaka, O.F. Hatipoglu, H. Takahashi, et al., Glycolaldehyde-derived advanced glycation end products promote macrophage proliferation via the JAK-STAT signaling pathway, Mol. Biol. Rep. (2023), https://doi.org/10.1007/s11033-023-08509-y.
[25] J. Raupbach, S.K. Müller, V. Schnell, S. Friedrich, A. Hellwig, T. Grune, et al., The effect of free and protein-bound Maillard reaction products N-ε-carboxymethyllysine, N-ε-fructosyllysine, and pyrraline on Nrf2 and NFκB in HCT 116 cells, Mol. Nutr. Food Res. 67 (18) (2023), https://doi.org/10.1002/mnfr.202300137.
[26] J.V. Valencia, M. Mone, C. Koehne, J. Rediske, T.E. Hughes, Binding of receptor for advanced glycation end products (RAGE) ligands is not sufficient to induce inflammatory signals: lack of activity of endotoxin-free albumin-derived advanced glycation end products, Diabetologia 47 (5) (2004) 844–852, https://doi.org/10.1007/S00125-004-1392-9/FIGURES/7.
[27] E. Birben, Ü.M. Şahiner, C.Ö. Kalayci, Determination of the effects of advanced glycation end products receptor polymorphisms and its activation on structural cell responses and inflammation in asthma, Turkish Journal of Medical Sciences 53 (1) (2023) 160–170, https://doi.org/10.55730/1300-0144.5569.
[28] M. Lappas, M. Permezel, G.E. Rice, Advanced glycation endproducts mediate pro-inflammatory actions in human gestational tissues via nuclear factor-κB and extracellular signal-regulated kinase 1/2, J. Endocrinol. 193 (2) (2007) 269–277, https://doi.org/10.1677/JOE-06-0081.
[29] A. Ohtsu, Y. Shibutani, K. Seno, H. Iwata, T. Kuwayama, K. Shirasuna, Advanced glycation end products and lipopolysaccharides stimulate interleukin-6 secretion via the RAGE/TLR4-NF-κB-ROS pathways and resveratrol attenuates these inflammatory responses in mouse macrophages, Exp. Ther. Med. (2017), https://doi.org/10.3892/etm.2017.5045 (accessed December 4, 2024).
[30] M. Shu, W. Cheng, X. Jia, X. Bai, Y. Zhao, Y. Lu, et al., AGES promote atherosclerosis by increasing LDL transcytosis across endothelial cells via RAGE/

NF-κB/caveolin-1 pathway, Mol. Med. 29 (1) (2023) 1–16, https://doi.org/10.1186/S10020-023-00715-5. FIGURES/7.
[31] C. Adamopoulos, C. Piperi, A.N. Gargalionis, G. Dalagiorgou, E. Spilioti, P. Korkolopoulou, et al., Advanced glycation end products upregulate lysyl oxidase and endothelin-1 in human aortic endothelial cells via parallel activation of ERK1/2-NF-κB and JNK-AP-1 signaling pathways, Cell. Mol. Life Sci. 73 (8) (2016) 1685–1698, https://doi.org/10.1007/S00018-015-2091-Z. FIGURES/4.
[32] C. Shen, Y. Ma, Z. Zeng, Q. Yin, Y. Hong, X. Hou, et al., RAGE-specific inhibitor FPS-ZM1 attenuates AGEs-induced Neuroinflammation and oxidative stress in rat primary microglia, Neurochem. Res. 42 (10) (2017) 2902–2911, https://doi.org/10.1007/s11064-017-2321-x.
[33] V. Kumar, T. Fleming, S. Terjung, C. Gorzelanny, C. Gebhardt, R. Agrawal, et al., Homeostatic nuclear RAGE-ATM interaction is essential for efficient DNA repair, Nucleic Acids Res. 45 (18) (2017) 10595–10613, https://doi.org/10.1093/nar/gkx705.
[34] V. Kumar, R. Agrawal, A. Pandey, S. Kopf, M. Hoeffgen, S. Kaymak, et al., Compromised DNA repair is responsible for diabetes-associated fibrosis, EMBO J. 39 (11) (2020), https://doi.org/10.15252/EMBJ.2019103477.
[35] Z. Han, M. Andrš, B.K. Madhavan, S. Kaymak, A. Sulaj, Z. Kender, et al., The importance of nuclear RAGE-Mcm2 axis in diabetes or cancer-associated replication stress, Nucleic Acids Res. 51 (5) (2023) 2298–2318, https://doi.org/10.1093/nar/gkad085.
[36] J. Mosquera-Sulbarán, A. Pedreáñez, Y. Carrero, C. Peña, Nuclear and cytoplasmic expressions of the receptor for advanced glycation end products (RAGE) in the rat central nervous system, Investig. Clin. 64 (4) (2023) 505–512, https://doi.org/10.54817/ic.v64n4a07.
[37] B. Liliensiek, M.A. Weigand, A. Bierhaus, W. Nicklas, M. Kasper, S. Hofer, et al., Receptor for advanced glycation end products (RAGE) regulates sepsis but not the adaptive immune response, J. Clin. Invest. 113 (2004), https://doi.org/10.1172/JCI200418704.
[38] T. Chavakis, A. Bierhaus, N. Al-Fakhri, D. Schneider, S. Witte, T. Linn, et al., The pattern recognition receptor (RAGE) is a Counterreceptor for leukocyte Integrins: a novel pathway for inflammatory cell recruitment, J. Exp. Med. 198 (10) (2003) 1507–1515, https://doi.org/10.1084/jem.20030800.
[39] Y. Gao, H. Wake, Y. Morioka, K. Liu, K. Teshigawara, M. Shibuya, et al., Phagocytosis of advanced glycation end products (AGEs) in macrophages induces cell apoptosis, Oxidative Med. Cell. Longev. (2017), https://doi.org/10.1155/2017/8419035.
[40] F. Sun, S. Suttapitugsakul, H. Xiao, R. Wu, Comprehensive analysis of protein glycation reveals its potential impacts on protein degradation and gene expression in human cells, J. Am. Soc. Mass Spectrom. 30 (12) (2019) 2480, https://doi.org/10.1007/S13361-019-02197-4.
[41] N. Takizawa, K. Takada, K. Ohkawa, Inhibitory effect of nonenzymatic glycation on ubiquitination and ubiquitin-mediated degradation of lysozyme, Biochem. Biophys. Res. Commun. 192 (2) (1993) 700–706, https://doi.org/10.1006/BBRC.1993.1471.
[42] X. Qiao, W. Li, Z. Zheng, C. Liu, L. Zhao, Y. He, et al., Inhibition of the HMGB1/RAGE axis protects against cisplatin-induced ototoxicity via suppression of inflammation and oxidative stress, Int. J. Biol. Sci. 20 (2) (2024) 784–800, https://doi.org/10.7150/ijbs.82003.
[43] H. Yang, H. Liu, Q. Zeng, G.H. Imperato, M.E. Addorisio, J. Li, et al., Inhibition of HMGB1/RAGE-mediated endocytosis by HMGB1 antagonist box a, anti-HMGB1 antibodies, and cholinergic agonists suppresses inflammation, Mol. Med. 25 (1) (2019) 1–13, https://doi.org/10.1186/S10020-019-0081-6/FIGURES/8.
[44] M. Watanabe, T. Toyomura, M. Tomiyama, H. Wake, K. Liu, K. Teshigawara, et al., Advanced glycation end products (AGEs) synergistically potentiated the proinflammatory action of lipopolysaccharide (LPS) and high mobility group box-1 (HMGB1) through their direct interactions, Mol. Biol. Rep. 47 (9) (2020) 7153–7159, https://doi.org/10.1007/S11033-020-05783-Y/FIGURES/4.
[45] E.C. Dullah, C.M. Ongkudon, Current trends in endotoxin detection and analysis of endotoxin–protein interactions, Crit. Rev. Biotechnol. (2017) 251–261, https://doi.org/10.3109/07388551.2016.1141393.
[46] A. Goode, V. Yeh, B.B. Bonev, Interactions of polymyxin B with lipopolysaccharide-containing membranes, Faraday Discuss. 232 (2021) 317–329, https://doi.org/10.1039/d1fd00036e.
[47] A. Boiko, A. Fiore, A. Hay, A.D. Troise, S. De Pascale, A. Scaloni, et al., The Glycation Database: From the Maillard Reaction in Foods to Biomolecular Insight, Abertay University, 2022.
[48] J.L.J.M. Scheijen, E. Clevers, L. Engelen, P.C. Dagnelie, F. Brouns, C.D. A. Stehouwer, et al., Analysis of advanced glycation endproducts in selected food items by ultra-performance liquid chromatography tandem mass spectrometry: presentation of a dietary AGE database, Food Chem. 190 (2016) 1145–1150, https://doi.org/10.1016/J.FOODCHEM.2015.06.049.
[49] J.L.J.M. Scheijen, M.P.H. van de Waarenburg, C.D.A. Stehouwer, C.G. Schalkwijk, Measurement of pentosidine in human plasma protein by a single-column high-performance liquid chromatography method with fluorescence detection, J. Chromatogr. B Analyt. Technol. Biomed. Life Sci. 877 (7) (2009) 610–614, https://doi.org/10.1016/j.jchromb.2009.01.022.
[50] A. Moysa, D. Hammerschmid, R.H. Szczepanowski, F. Sobott, M. Dadlez, Enhanced oligomerization of full-length RAGE by synergy of the interaction of its domains, Sci. Rep. 9 (1) (2019), https://doi.org/10.1038/s41598-019-56993-9.
[51] H.E. Zenker, A. Ewaz, Y. Deng, H.F.J. Savelkoul, R.J.J. Van Neerven, N. De Jong, et al., Differential effects of dry vs. wet heating of β-lactoglobulin on formation of sRAGE binding ligands and sIgE epitope recognition, Nutrients 11 (6) (2019), https://doi.org/10.3390/nu11061432.